

Biosorption of phosphorus, total suspended and dissolved solids by dried *Phragmites australis*: isotherm, kinetic and interactive response surface methodology (IRSM) in oil and soap-derivatives industrial wastewater

Ghada Heikal^{a,*}, Abeer El Shahawy^b

^aEnvironmental Engineering Department, Faculty of Engineering, Zagazig University, PO Box 44519, Zagazig, Egypt, emails: reemhatem2006@hotmail.com, ghhekal@zu.edu.eg

^bDepartment of Civil Engineering, Faculty of Engineering, Suez Canal University, PO Box 41522, Ismailia, Egypt, email: ahmedabeer12000@yahoo.com

Received 2 March 2018; Accepted 24 September 2018

ABSTRACT

Releasing phosphorus (P) in contaminated water straightforwardly into the sea-going condition prompts asset misfortune and simulates eutrophication in existence of nitrogen. In this manner, expelling P from squander streams is basic. In this investigation, *Phragmites australis* as an ease biosorbent was intended to viably adsorb P, total suspended solids (TSS), and total dissolved solids (TDS) from genuine modern wastewater. *P. australis* was portrayed through Fourier-transform infrared spectroscopy examination, trailed by SEM investigation, studying the influenced parameters, lastly, isotherm and active adsorption explore additionally occurred. *P. australis* was found to have favored P, TSS, and TDS biosorption capacity. The Freundlich isotherm fits the biosorption procedure satisfactorily of phosphorus, TSS, and TDS with $R^2 = 0.998, 0.999, \text{ and } 0.999$, respectively. Then again, the pseudo-first-order kinetics demonstrates fits biosorption procedure of TSS with $q_e = 117.436 \text{ mg g}^{-1}$ however, pseudo-second-order kinetics shows well fits the biosorption of P and TDS with $q_e = 6.5189 \text{ and } 1,250 \text{ mg g}^{-1}$. Hence, *P. australis* is an ecological neighborly and minimal effort sorbent for P evacuation.

Keywords: *Phragmites*; Phosphorus; TSS; TDS; Kinetics; Isotherm; IRSM.

1. Introduction

Phosphorus (P) is a basic macroelement that has a significant effect on the growth of aquatic plants. Its existence in large amounts as phosphate (PO₄-P) in the amphibian biological communities can stimulate the eutrophication process and thus deteriorates the water quality. Additionally, high concentrations of phosphate can cause the rapid growth of algal sprouts and the depletion of oxygen in the water bodies, which may result in negative effects on the amphibian living beings. Human activities such as the disposal of creature excrement and compost into the soil or the release of industrial, sewage, and horticultural wastewater are

reasons of increasing the phosphate loadings in the surface water [1]. Several techniques for removing phosphorus have been developed such as biological [2] and physical-chemical [3] techniques. Biological process such as enhanced biological phosphorus removal (EBPR) and biofilm [4] is very essential for the removal of phosphorus. On the other hand, these microorganisms are affected significantly by the water potentials including carbon source [5] and temperature [6]. Additionally, precipitation is an expensive physical-compound process and produces large amount of slime which must be managed appropriately [7]. Other techniques such as electrocoagulation and electrodialysis can be used for phosphorus removal. However, their high running cost constrained their wide application [8].

* Corresponding author.

On the other hand, adsorption by utilizing minerals is considered as an effective, straightforward, and simple technique for PO₄-P expulsion even at low phosphate fixations. In any case, the alteration of characteristic minerals is expected to alter their surface charge from negative to positive and to empower them to adsorb phosphate anions [9]. Various altered mineral adsorbents have been tried by [1] for phosphate expulsion at low (<10 mg L⁻¹), medium (10–100 mg L⁻¹), and high (>100 mg L⁻¹). In any case, there is a specific enthusiasm for adsorbents which can effectively treat arrangements of low introductory P fixations and show low lingering focuses in the request of ppb (μg L⁻¹) in the effluents [10]. These concentrations are required from the legislations with reference to municipal wastewater treatment ranging from 0.5 to 2 mg L⁻¹ before wastewater is discharged into water sources [11]. Egyptian Environmental Regulations allowed that the ultimate phosphorus concentration is 5 mg L⁻¹ before the wastewater is discharged into surface water source. A vital parameter in sorption process is the adsorbent molecule size, which is identified with adsorption limit, kinetics and partition of the adsorbent from the fluid stage [12]. The fundamental aspect that impedes the efficient utilization of these elective procedures is the synthetic alterations of these substances, which increase the cost of presenting buildups and are naturally inconsistent.

Total dissolved solids (TDS) are inorganic and exist mostly in ionic shape. These days, the expulsion of disintegrated solids from industrial wastewater is under research for the ecological designers. Inorganic parts of disintegrated solids are harder to evacuate by organic procedures. There are a few other treatment strategies, for example, synthetic precipitation, adsorption, electrophoresis, softening, and switch osmosis, rehearsed to expel disintegrated solids from wastewater. Nevertheless, every technique has its own particular restrictions. As, regardless of the way that clearing of various parts of TDS by engineered precipitation is a revealed development, it requires a capable solid separation system and legitimate solid waste disposal facilities [13].

Phragmites australis, commonly known as reed, is used in the present study. It is an extensive perpetual grass found in wetlands all through calm and tropical locales of the world. It can mature up to 6 m high and is seemingly perpetual and contains high content of lignin and cellulose. Properties of *P. australis* do not just give a possibly economical material to wastewater treatment but in addition it helps surface adjustment by methods for extraordinary quantities of hydroxyl gatherings (OH) on its surface. *P. australis* has been utilized for quite a long time for the evacuation of overwhelming metals and metalloids from amphibian frameworks and wastewater removal [14]. However, to the best of the authors knowledge, previous studies did not examine the evacuation of (phosphorous, total suspended solids (TSS), and TDS). Depending upon the realities that the examinations on crude *P. australis* are restricted and the favorable circumstances on utilization of this amphibian plant (simple access or minimal effort generation) are exceptionally extensive as far as common sense potential with future imminent. *P. australis* has high potential because of the following: (1) its dense growth, (2) spreading root system, and (3) its adaptability to withstand hostile environment, alternating wet and dry conditions, elevated CO₂ and high temperature which is conferred by several factors

such as change of carbon-trapping mechanism, microbial association, and biochemical adaptations. All of these factors make it one of the best water clearing plants for the tropics. *P. australis* played an important role in land reclamation. In polders reclaimed from the sea, it was shown as the first crop because of its salt tolerance. *P. australis* has been the recorded plant among the ecological engineers for its application in constructed wetlands. Many review papers concentrated on *P. australis* have emphasized the importance of using this grass in environmental protection engineering. The rhizomes of *P. australis* are highly preserved, as these remain dormant in the soil and sediments, which help provide protection from frostiness and fire [15].

The objective of the work was set to investigate the effectiveness of *P. australis* as a biosorbent for the removal of phosphorous, TSS, and TDS from oil and soap derivatives industrial wastewater. The main objectives of this study are to: (1) characterize the synthesized biosorbent by scanning electron microscopy (SEM) and Fourier-transform infrared spectroscopy (FTIR); (2) systematically evaluate the influences of various experimental parameters on adsorption performance; and (3) reveal the sorption isotherms and kinetics of phosphorous, TSS, and TDS onto dried biomass *P. australis*. This study seeks also to find the correlation between the experimental parameters and phosphorous, TSS, and TDS removal to find the parameters that have the greatest influence on phosphorous, TSS, and TDS removal efficiency.

2. Materials and methods

2.1. Collection and composition of oil and soap derivatives industrial wastewater

Different soap and oil derivatives industrial wastewater samples were taken from Misr oils and soap derivatives Industries Company, Zagazig City, Sharkiah, Egypt. The main characteristics of soap and oil derivatives wastewater are listed in Table 1. The samples were taken at different times through a year and measured parameters were recorded in its mean values. All analyses were conducted according to the Standard methods for the examination of water and wastewater. Phosphorus concentrations were measured using stannous chloride method. Standard concentrations of phosphorus were calibrated using spectrophotometer (Spekol UV/VIS) at wavelength 705 nm and plotted as absorbance versus phosphorus concentration in Fig. 1 as a calibration curve of phosphorus concentrations. Total suspended solids were measured after filtration and drying the sample at 103°C–105°C. Settleable solids were measured by the gravimetric method. Total dissolved solids were measured for the filtered liquid by the gravimetric method. Nitrogen concentration was not applicable in this industrial wastewater effluent of soap and oil derivatives effluent. pH of aqueous solution was adjusted to the desired value by the addition of NaOH (0.1 M) or HCl (0.1 M).

2.2. Biosorbent preparation and its characterization

Phragmites australis (reeds) were collected from EL Agha canal at Zagazig town, situated on the Nile Delta region

Table 1
The characteristics of the used oil and soup industrial wastewater

Parameter	Value (ppm)
pH	4.3
BOD (ppm)	20,900
COD (ppm)	43,600
SS (ppm)	1,850
DS (ppm)	17,400
O&G (ppm)	8,900

Nitrogen concentration < 0.39 ppm (N/A).

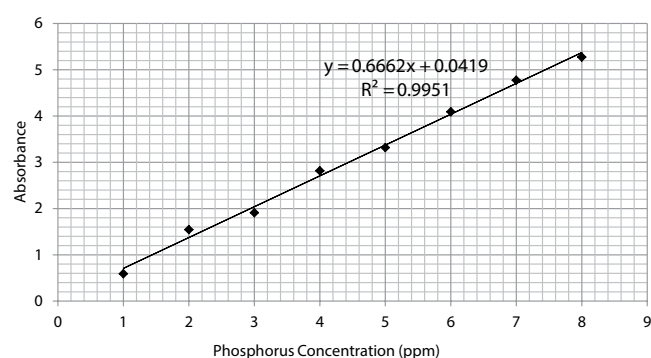


Fig. 1. Calibration curve of phosphorus concentrations.

of Egypt. The harvested plants were dissected, washed with 1% HCl, and then rinsed with deionized water to remove any material adhering to plant parts. After that, the plants were placed in an oven (Shimaden) at 70°C for 48 h to get oven-dry weight. Plant samples were finely crushed, grinded, and then sieved by sieve analysis to prepare the desired particle size which is 0.15 mm at sieve # 150. The characteristics of raw *P. australis* biomass are shown in Table 2.

2.3. Instruments

The values of pH were determined using pH meter (AD1000). All the chemicals used in the study were analytically pure and purchased from local suppliers, Egypt. Stainless-steel sieve analysis (Standard Sieves Dual Manufacturing Co., USA) was used to obtain definite particle size of the biosorbent. All physic-chemical analyses were performed according to the standard methods for examination of water and wastewater (APHA, 1998). The surface of the studied biosorbent, before and after biosorption process, was analyzed and photographed using a Scanning Electron

Microscope (JEOL JSM-6510LV SEM, USA) equipped with energy dispersive x-ray spectroscopy (EDAX). Fourier Transform Infrared (FT-IR) Spectrometer (JASCO 4100, USA) was used to detect the main functional groups responsible for organic load biosorption. The spectra were collected using the FT-IR instrument equipped with diffuse reflectance accessory within wavenumber range of 400–4,000 cm⁻¹.

2.4. Batch biosorption procedure

The first part of this study aimed at determining the optimum operating parameters for organic load biosorption. This included the effects of pH 4–9, biomass dosage level 0.5–3.5 g per 250 mL, contact time 10–180 min, agitation speed 120–300 rpm on selected dried biomass and plant particle size = 0.15 mm on the organic load removal and uptake capacity. All experiments were conducted in triplicate using agitation speed 150 rpm at constant room temperature of 25°C ± 3°C, for every kinetic experiment, 250 mL of oil and soup derivatives wastewater. The second part of this study was used to determine the effect of initial phosphorous, TSS, and TDS concentrations by dried *P. australis* biomass. phosphorus, TSS, and TDS concentrations were varied from 20 to 100, 350 to 1,850, and 3,480 to 17,400 mg L⁻¹, respectively at optimum adsorbent dose, contact time, pH, and agitation speed achieved from the first part. The third part of the present study examined the efficiency of studied biosorbent for removal of TSS and TDS from real wastewater samples collected from olive oil mill industrial wastewater produced from factory at the North Sinai governorate in Egypt.

2.5. Biosorption isotherm models

The adsorption isotherms are harmony conditions that regularly express the measure of adsorbate on the adsorbent as a component of its concentration. The linear form of the Langmuir isotherm refers to Langmuir equation [16]. The logarithmic form of the Freundlich model refers to Freundlich equation [17].

2.6. Kinetic studies

The adsorption rate of phosphorus, TSS, and TDS was studied at different time intervals for 180 min using 100, 1,850, and 17,400 mg L⁻¹ initial concentrations respectively at the optimum value of adsorbent dose. The modeling of phosphorus, TSS, and TDS adsorption kinetics for *P. australis* was checked by two common models using the pseudo-first-order and pseudo-second order [18] refer to pseudo-first-order and pseudo-second-order equations.

Table 2
Characteristics of *Phragmites australis* dried biomass

Proximate analysis (wt.%)	Leaves	Stems	Lignocellulosic composition (wt.%)	Leaves	Stems
Ash	4.5	5.1	Cellulose	39.5	42.7
Moisture	3.7	4.2	Lignin	29.69	27.27
Volatile	42.0	36.1	Hemicellulose	23.61	23.73
Fixed carbon	49.8	54.6	Extractives	7.2	6.3

2.7. Intraparticle diffusion model

The intraparticle diffusion model describes adsorption processes, where the rate of adsorption depends on the speed at which adsorbate diffuses toward adsorbent (i.e., the process is diffusion controlled), which is proposed by [19].

2.8. Statistical analysis

The numerical data in this study using the single analysis of variance (ANOVA) and the simple correlation analysis. One-way ANOVA (at a significance level of 0.05) was applied to assess the removal efficiencies of the biosorption capacity.

Interactive response surface methodology (IRSM) is a combination of statistical techniques used for designing experiments, generating models, and estimating the effects of variables. The IRSM generates simulated data at combinations of independent variables specified by a designed experiment. Recently, IRSM has been employed for modeling and optimizing a variety of wastewater treatment technologies [20]. In the current study, the IRSM was based on a pure-quadratic regression model Eq. (1) to fit the experimental results.

$$Y = \beta_0 + \beta_1 x_1 + \beta_2 x_2 + \beta_3 x_3 + \beta_4 x_4 + \beta_5 x_5 + \beta_6 x_1^2 + \beta_7 x_2^2 + \beta_8 x_3^2 + \beta_9 x_4^2 + \beta_{10} x_5^2 \quad (1)$$

where Y is the predicted response of P, TSS, and TDS removal efficiency (%); concentration 370:1,850, 3,480:1,7400, and 20:100, mg L⁻¹, respectively; x_1 is biomass dosage (0.5–3.5 g);

x_2 is agitation speed (120–300 rpm); x_3 is contact time (10–180 min); x_4 is pH (4–9); x_5 is initial TSS, TDS, and P; β_0 is the model intercept; $\beta_1, \beta_2, \beta_3, \beta_4$ and β_5 are the linear coefficients of x_1, x_2, x_3, x_4 and x_5 , respectively; $\beta_6, \beta_7, \beta_8, \beta_9$ and β_{10} are the quadratic coefficients of x_1, x_2, x_3, x_4 and x_5 , respectively.

3. Results and discussion

3.1. Characterization studies of raw and polluted *P. australis* dried biomass

3.1.1. FTIR spectroscopy

FTIR spectra of both raw and adsorbent (loaded) plant biomass show that at 3,850.18/3,848.26, 3,753.76/3,745.08 cm⁻¹ ignore overtone, this initially because at this value it is too weak to be a fundamental. The O–H stretching vibrations between 3,433.64 and 3,400.85 cm⁻¹ indicating the presence of alcohols and phenols are present in the structure (Fig. 2). The absorption bands at 2,923.56 cm⁻¹ for raw and polluted plant biomass can be assigned to aromatic ring stretching (phenolic groups), respectively. The C=O stretching vibrations at 1,627.63 and 1,608.34 cm⁻¹ denoting the presence of the carbonyl groups refer to ketones, phenols, carboxyl acids, and aldehydes [21]. The bands appearing around the region at 1,102.12 and 1,103.08 cm⁻¹ represents C–H and C–OH stretching vibrations, respectively, which are due to the several functional groups present on the plant biomass and the peaks at 794.528/788.743 and 602.646/597.825 cm⁻¹ are associated with bending vibrations of CH₃, CH, and CH. The peak in raw *P. australis* was slightly shifted after COD, BOD, and Oil & Grease biosorption. The results reveal that a large

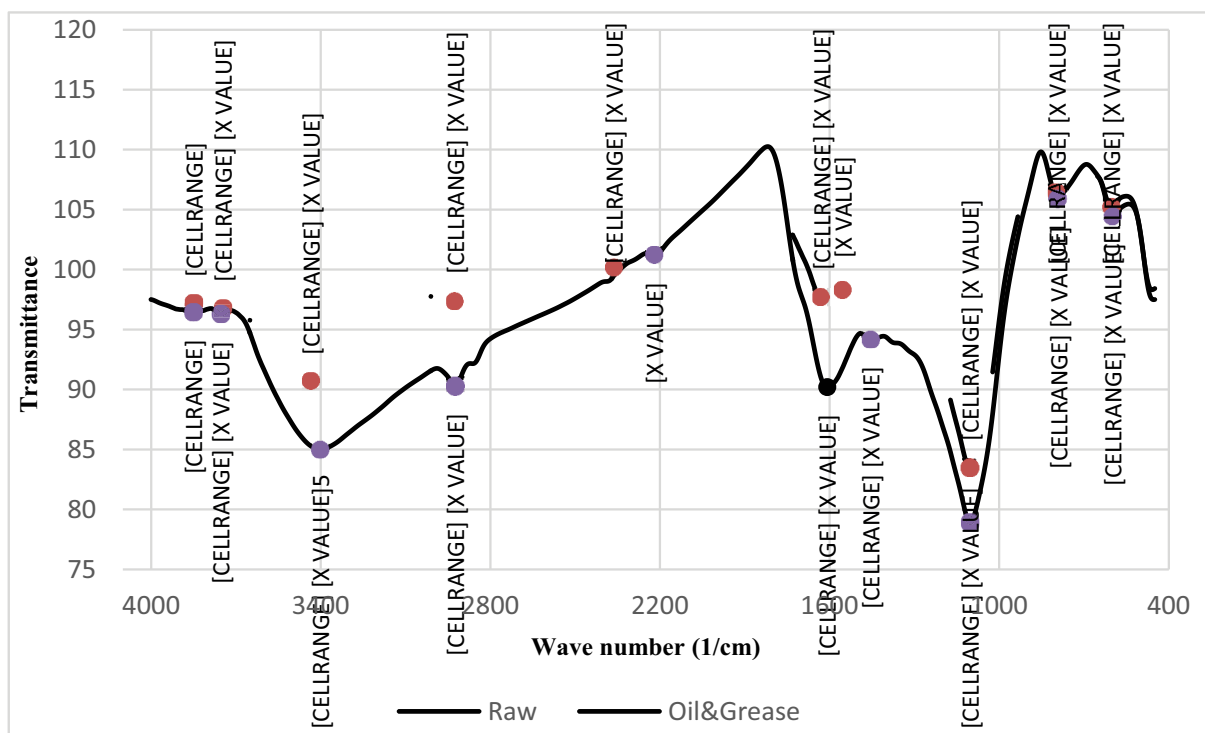


Fig. 2. FTIR spectrum of *Phragmites australis* dried biomass before and after adsorption.

amount of chemical functional groups was preserved and generated on the surface of *P. australis*, which might enhance its adsorptive properties [22].

3.1.2. Scanning Electron Microscopy studies

The overall morphology and microscopic porous structure of the samples can be clearly seen from SEM images, as illustrated in Figs. 3–6. In this study, SEM photomicrographs of the organic loads and *P. australis* magnification power 2,500 \times and 1,000 \times showed the morphological changes onto the *P. australis* surface after organic loads adsorption. SEM micrographs of the organic loads (Figs. 3 and 6) show that the surfaces of both raw and dried biomass are fluffy and rough. Figs. 3 and 4 shows the SEM micrographs of raw dried powder of *P. australis* containing irregular particles in the range of few micrometers to few hundred micrometers. The enhanced pictures demonstrate that some bigger squares contain general channel exhibits, and the dividers of the channels contain numerous bigger pores. This shows some portion of the channel structures of the first reed were safeguarded subsequent to drying the biomass.

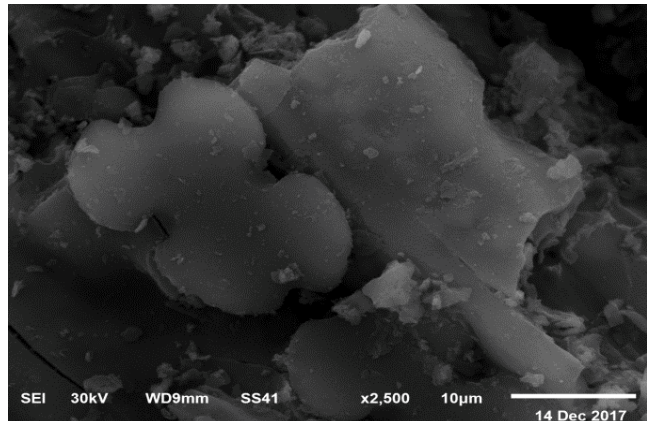
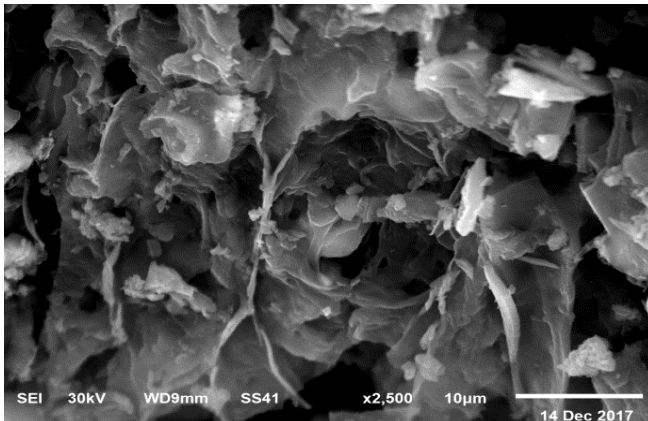
It was also observed that the surface of the raw dried biomass is cleaner than the surface of dried biomass after adsorption of the organic loads of TSS, TDS, and phosphorus.

As seen in Figs. 5–6, the surface morphology of the dried *P. australis* biomass varied and organic loads molecules accumulated on the biomass surface, indicating that the organic load adsorption had occurred at the surface.

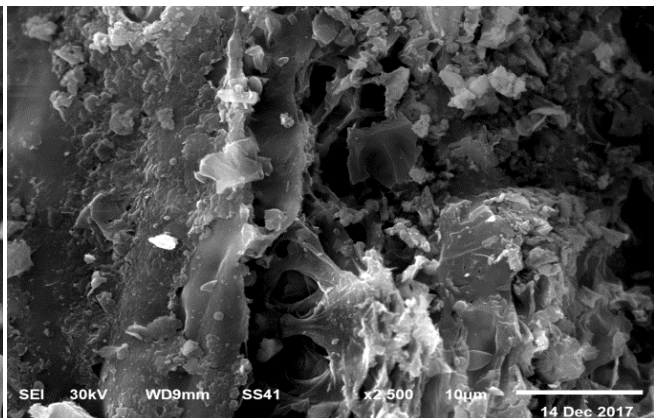
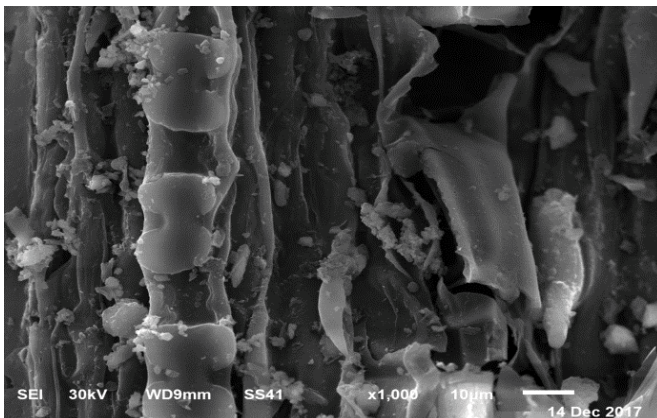
As presented in Figs. 5–6, the organic loads particles formed aggregates of various shapes and sizes. After adsorption of TSS, TDS, and phosphorus, pores ended up undetectable in light of the fact that the outer biomass surface has been covered by the organic load. Examination with SEM demonstrated high fondness of *P. australis* to the immediate natural burdens, affirming the adsorption procedure.

3.2. Effective dosage of *P. australis* biosorbent

The effect of biomass dosage on P, TSS, TDS biosorption was carried out at 100, 1,850, and 17,400 mg L⁻¹ respectively, at contact time = 20 min, pH = 4, and agitation speed = 150 rpm. The effect of *P. australis* dosage is shown in Fig. 7. The percentage removal of P, TSS, TDS increased rapidly from 14% \pm 0.200% to 45% \pm 0.000%, 15.68% \pm 0.220% to 43.03% \pm 0.410% and from 11.95% \pm 0.002% to 40.11% \pm 0.568% for P, TSS, TDS respectively, with the amount of added *P. australis* from 0.5 to 3.5 g per 250 mL (r 0.981, p 0.000), (r 0.969, p 0.000), and (r 0.968, p 0.000) for P, TSS, and TDS, respectively. The removal percentage increased with increase in dosage of



Figs. 3,4. SEM micrographs of raw dried *P. australis* biomass at magnification power 2,500 \times .



Figs. 5,6. Photos (3) and (4) SEM micrograph of dried *P. australis* biomass after adsorption at magnification power 1,000 \times and 2,500 \times .

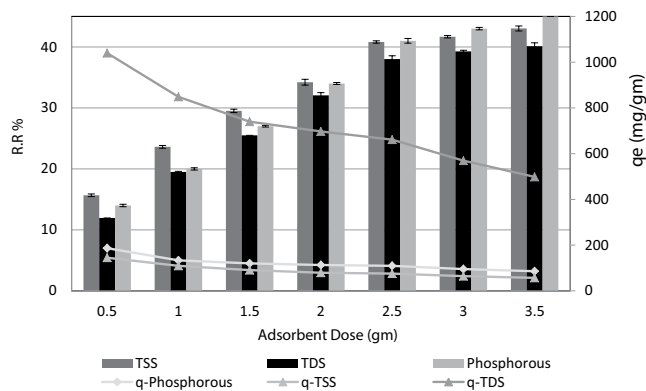


Fig. 7. Effect of adsorbent dose on the removal efficiency and the adsorption capacity of TSS, TDS and phosphorous at contact time = 120 min, pH = 4, and agitation speed = 150 rpm.

P. australis. However, at high adsorbent dosage between 12 and 14 g L⁻¹, the removal rate of P, TSS, TDS remained nearly constant. This may be attributed to the fact that there are many sites that are available through the adsorption process leading to a low ratio between the P, TSS, and TDS molecules to adsorbent dosage [23]. Additionally, an increase in biosorbent dose from 2 to 14.0 g L⁻¹ negatively affected the q_e ($r = -0.908$, $p = 0.005$), ($r = -0.945$, $p = 0.001$), and ($r = -0.968$, $p = 0.000$) for P, TSS, and TDS, respectively, which recorded the least value of 3.214 ± 0.026 , 56.857 ± 0.265 , and 498.57 ± 2.353 mg g⁻¹ at 14.0 g L⁻¹ (3.5 g per 250 mL) for P, TSS, and TDS, respectively. The relationship between uptake and dosage appears in contrast to the trend of phosphorus removal for both sorbents. This indicates a decrease in adsorption capacity per unit mass of sorbent with the increase in sorbent dosage, potentially mitigating to some extent the trend observed in increasing removal efficiency with sorbent dosage. The optimum adsorbent dosage for P, TSS, and TDS removal from aqueous solution by *P. australis* was 14 g L⁻¹ (3.5 g per 250 mL).

3.3. Effect of mixing time

The effect of contact time on P, TSS, and TDS biosorption was carried out at 100, 1,850, and 17,400 mg L⁻¹, respectively, at pH = 4, and agitation speed = 150 rpm. As shown in Fig. 8, P, TSS, TDS removal gradually increased from 27% ± 0.382% to 80% ± 0.754%, from 15.89% ± 0.145% to 81.62% ± 0.003% and from 11.75% ± 0.112% to 78.11% ± 0.740%, respectively, with an increase in contact time from 10 to 120 min ($r = 0.907$, $p = 0.002$), ($r = 0.885$, $p = 0.004$), and ($r = 0.882$, $p = 0.004$) for P, TSS, and TDS, respectively. Similar behavior was observed for q_e , which enhanced to 5.714 ± 0.050 , 107.857 ± 1.523 , and 970.714 ± 0.003 mg g⁻¹ for both P, TSS, and TDS, respectively with the contact time up to 120 min ($r = 0.907$, $p = 0.002$), ($r = 0.885$, $p = 0.004$), and ($r = 0.882$, $p = 0.004$) for P, TSS, and TDS, respectively. It was found that removal of P, TSS, and TDS increased with prolonging the contact time until attainment an equilibrium value of 120 min. In the initial stage (<120 min), the P, TSS, and TDS removal efficiency were enhanced, since there were many vacant active binding sites on the biosorbent surface. As time proceeded, the biosorbent was filled with P, TSS, and TDS retained and the adsorption rate decreases

and the process tends toward the steady state because of the gradual occupancy of the active binding sites until they were exhausted. The adsorption capacity of P, TSS, and TDS onto *P. australis* are in agreement with the structural properties of this material. It has been reported that the duration for equilibrium achievement for P, TSS, and TDS biosorption onto *P. australis* was 120 min.

3.4. Effect of solution pH

The pH estimation of the arrangement amid adsorption significantly affects the surface qualities of the adsorbent particles. It influences the surface charge of the biosorbent as well as the level of ionization of the natural substances introduced in the arrangement and the separation of utilitarian gatherings on the dynamic locales of the sorbent. The P, TSS, and TDS removal capacity of *P. australis* at various pH values was evaluated at 25°C with 100, 1,850, and 17,400 mg L⁻¹ respectively, at contact time = 120 min, agitation speed = 150 rpm, and biosorbent dose = 14 g L⁻¹ (3.5 g per 250 mL). Fig. 9 shows that the pH value of the solution greatly influenced the phosphorus capacity of *P. australis*. The amount of P, TSS, and TDS removal increased gradually from 80% ± 0.754% to 87% ± 0.000%, from 81.62% ± 0.001% to 93.51% ± 0.88% and from 78.1% ± 0.366% to 90.22% ± 0.422% respectively, with an increase in pH from 4 to 7 ($r = 0.994$, $p = 0.006$),

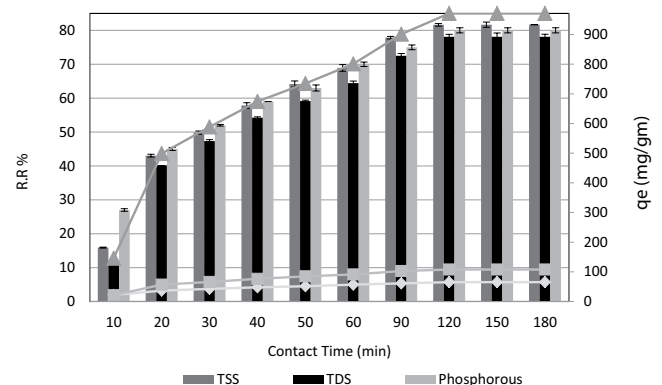


Fig. 8. Effect of contact time on the removal efficiency and the adsorption capacity of TSS, TDS and phosphorous at adsorbent dose = 3.5 g, pH = 4, and agitation speed = 150 rpm.

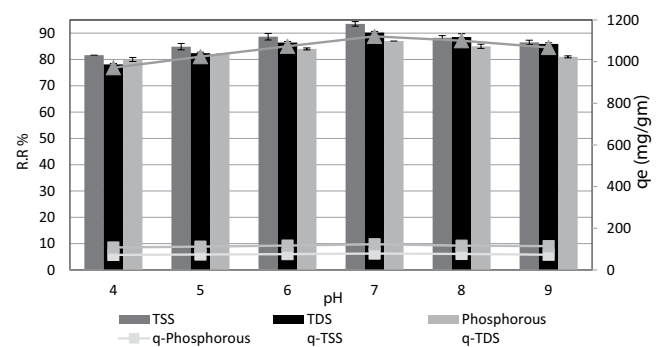


Fig. 9. Effect of pH on the removal efficiency and the adsorption capacity of TSS, TDS and phosphorous at adsorbent dose = 3.5 g, contact time = 120 min, and agitation speed = 150 rpm.

(r 0.995, p 0.004), and (r 1.00, p 0.00) for P, TSS, and TDS, respectively. Similar behavior was observed for q_e , which enhanced to 6.214 ± 0.059 , 123.57 ± 0.001 , and $1,121.4 \pm 5.286$ mg g^{-1} with pH up to 7 (r 0.994, p 0.006), (r 0.996, p 0.004), and (r 1.00, p 0.00) for P, TSS, and TDS, respectively. With increasing pH values P, TSS, and TDS sorption capacity decreased at a pH value above 7.0–9. The P, TSS, and TDS sorption capacity dropped to 81%, 86.49%, and 85.91% with (r -0.982, p 0.121), (r -0.960, p 0.182), and (r -0.993, p 0.077), respectively. In the same manner q_e dropped to 5.786, 114.29, and 1,067.8 mg g^{-1} at pH = 9 (r -0.982, p 0.121), (r -0.960, p 0.182), and (r -0.993, p 0.077) for P, TSS, and TDS, respectively, which indicated that *P. australis* may work well in neutral solutions but not in alkaline solutions. This finding was in agreement with previous results reported by other researchers using slag and palygorskite ash as adsorbents. The pH dependency of P, TSS, and TDS removal is related to the dissolution of cations from the adsorbent, overall charge of the adsorbent and polyprotic nature of phosphate. The pH of solution has an impact on the speciation of phosphate ions in solution. Between pH of 3 and 7, the predominant species is H_2PO_4^- and normally carries negative charge. At the point when the pH increased, the measure of phosphorus adsorbed strongly diminished, which was fundamentally ascribed to the high pH values. High pH values could make the surface convey more negative charges, in this way bringing about expanded repugnance of the contrarily charged phosphate in the arrangement [24]. Conceivable clarifications for these outcomes include: in acidic conditions, biosorbent pores are extended; the surface will be encompassed by the hydrogen particles, which upgrades the associations between the natural substances and restricting destinations through alluring powers. In antacid conditions, OH-in arrangement, which rivals the PO_4^{3-} species, ends up higher bringing about electrostatic aversion because of the diminishment of electrostatic power of fascination between the oppositely charged adsorbate particles and the coupling adsorbent locales. Insoluble base medium, concoction precipitation covers the area position throughout adsorption [25].

3.5. Effect of mixing speed

Experiments were conducted to investigate the effect of stirring speed on P, TSS, and TDS adsorption onto the *P. australis* for initial concentration of 100, 1,850, and 17,400 mg L^{-1} , respectively, with 14 g L^{-1} of biosorbent dose at 120 min, at $25^\circ\text{C} \pm 3^\circ\text{C}$, stirring speeds in the range of 120–300 rpm. The results are given in Fig. 10. As can be seen from this figure, there is a rise in P, TSS, and TDS removal rate with increasing the agitation speed. The maximum removal efficiency ($87\% \pm 1.230\%$, $93.51\% \pm 1.326\%$, and $90.22\% \pm 0.847\%$) was recorded at agitation speed from 120 to 150 rpm for P, TSS, and TDS, respectively, after which significant decrease was noticed. When agitation speed was elevated from 150 to 300 rpm r -0.987, p 0.013 for P, r -0.950, p 0.05 for TSS, and r -0.942, p 0.058 for TDS. Moreover, q_e showed a dramatic increase from 4.786 ± 0.021 to 6.214 ± 0.088 mg g^{-1} for P, from 105.93 ± 1.495 to 123.57 ± 0.579 mg g^{-1} for TSS, and from 974.57 ± 4.597 to $1,121.4 \pm 10.572$ mg g^{-1} for TDS with an elevation in agitation speed from 120 to 150 rpm, respectively. However, further increase in agitation speed from 150

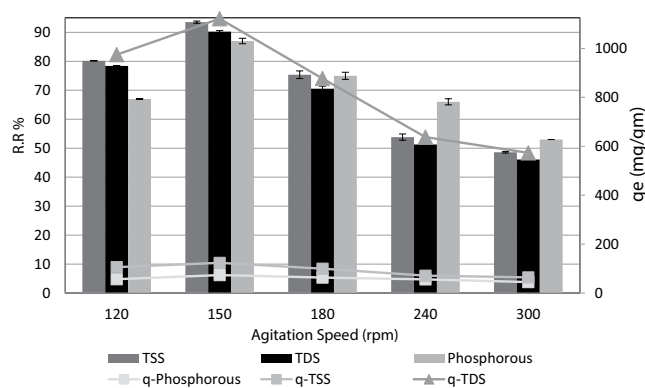


Fig. 10. Effect of agitation speed on the removal efficiency and the adsorption capacity of TSS TDS and phosphorous at adsorbent dose = 3.5 g, contact time = 120 min, and pH = 7.

to 300 rpm showed a decrease in the q_e to 3.786, 64.214, and 572.93 mg g^{-1} with r -0.987, p 0.013 for P, r -0.950, p 0.05 for TSS, and r -0.942, p 0.058 for TDS, respectively. This may be interpreted to the dispersal of the adsorbent particles. This is due to the fact that the adsorption process is mass transfer driven. It is believed that the liquid side mass transfer resistance controls the process. Thus, the adsorption rate increases with bulk motion [26]. With increasing blending speed, the adsorption limit of phosphate diminished. This shows the dispersion of the phosphate particle from the solution for the surface of the adsorbent and into the pores happens easily and rapidly. This is due to the powder shape of the adsorbents. Restabilization of suspended strong will happen, when the blending speed is quick. This marvel can be obviously observed for readings of suspended strong for blending speed more 150 rpm [27]. *P. australis* showed the most stringent changes, which proves that *P. australis* is a good binder.

3.6. Effect of initial concentration of (P, TSS, and TDS)

The effect of P, TSS, and TDS concentration 20–100, 370–1,850, and 3,480–17,400 mg L^{-1} for P, TSS, and TDS, respectively, on biosorption process was investigated with pH of 7.0, biosorbent dosage of 14 g L^{-1} and particle size of 0.15 mm for 120 min at agitation speed 150 rpm. The results in Figs. 11(a)–(c) revealed that increasing the initial P, TSS, and TDS concentration from 20 to 100, from 370 to 1,850, and from 3,480 to 17,400 mg L^{-1} , respectively, could linearly decline the P removal from $89.54\% \pm 0.848\%$ to $87\% \pm 0.820\%$, TSS removal from $96.43\% \pm 0.905\%$ to $93.51\% \pm 1.325\%$ and TDS removal from $93.54\% \pm 0.886\%$ to $90.22\% \pm 1.273\%$ with (r -0.984, p 0.002), (r -0.979, p 0.004), (r -0.984, p 0.002) for P, TSS, and TDS, while q_e elevated from 1.28 ± 0.018 to 6.21 ± 1.055 , from 25.49 ± 0.361 to 123.57 ± 1.744 and from 232.51 ± 1.092 to $1,121.36 \pm 0.003$ mg g^{-1} with (r 1, p 0.00) the same for P, TSS, and TDS, respectively. It was evident that the increase in initial concentration of P, TSS, and TDS resulted in a decrease in percent removal and an increase in the uptake capacity. The removal rate of P, TSS, and TDS from solution decreases with increase of the P, TSS, and TDS initial concentration, and the amount of P, TSS, and TDS adsorbed by the adsorbent increases with increase of the initial concentration of P, TSS, and TDS in the solution. The higher

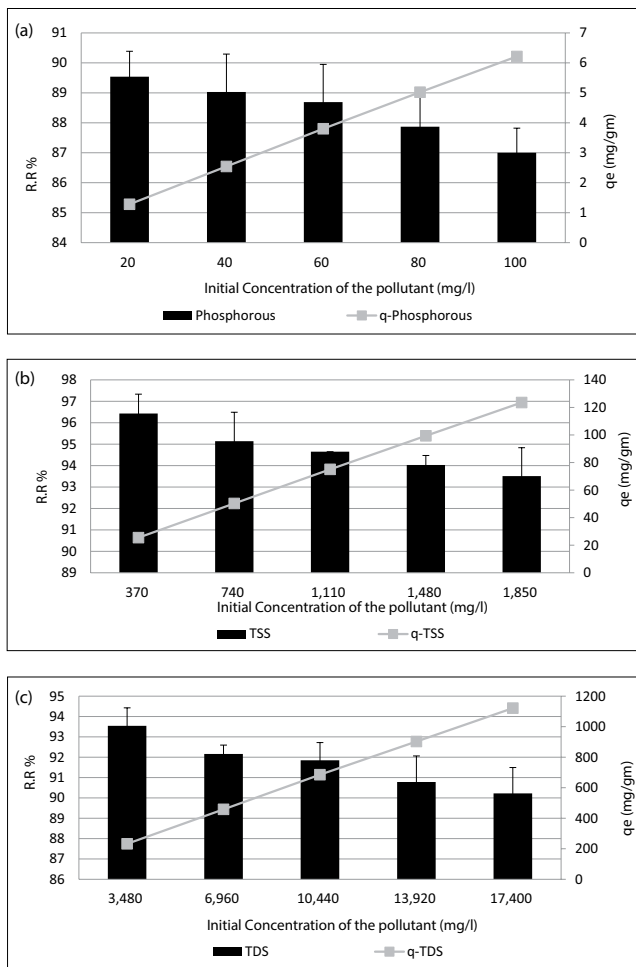


Fig. 11. (a) Effect of initial concentration on the removal efficiency and the adsorption capacity of Phosphorous at adsorbent dose = 3.5 g, contact time = 120 min, pH = 7, and agitation speed = 150 rpm, (b) Effect of initial concentration on the removal efficiency and the adsorption capacity TSS at adsorbent dose = 3.5 g, contact time = 120 min, pH = 7, and agitation speed = 150 rpm, (c) Effect of initial concentration on the removal efficiency and the adsorption capacity of TDS at adsorbent dose = 3.5 g, contact time = 120 min, pH = 7, and agitation speed = 150 rpm.

initial concentration of P, TSS, and TDS with fixed amount of adsorbent will result in a higher equilibrium concentration of P, TSS, and TDS in the solution, which contributes to a higher amount of P, TSS, and TDS adsorbed by the adsorbent. At low P, TSS, and TDS concentrations, the number of ions competing for the available active sites in the biomass decreased, and thus, there was sufficient surface area to accommodate P, TSS, and TDS available in the solution. Also, the decrease of vacant adsorption sites in the surface area is one of the reasons for the decrease because the ratio between P, TSS, and TDS molecules to the adsorbent dosage increases with the increase of the initial concentration.

3.7. Adsorption isotherm

The adsorption isotherm indicates how the adsorbate molecules are distributed between the liquid phase and the

solid phase. In order to evaluate the adsorption capacity of *P. australis* powder, the P, TSS, and TDS adsorption equilibrium was studied as a function of P, TSS, and TDS concentration. The experiment was conducted under the same conditions that produced the maximum P, TSS, and TDS removal. Therefore, the equilibrium study was performed under the following conditions: pH 7.0; adsorbent dose 14 mg L⁻¹ in solution; at -25°C ± 3°C; contact time of 120 min at 150 rpm. The equilibrium adsorption data for the adsorption of P, TSS, and TDS by *P. australis* were analyzed by the Langmuir and Freundlich isotherm equations.

3.7.1. Langmuir isotherm

The linear form of the Langmuir isotherm model is described as the values of Langmuir parameters, q_{max} and K_L as shown in Table 3. Values of q_{max} , K_L and regression coefficient R_2 are 250, 2,500, and 23,981 mg g⁻¹, 0.00764, 0.000426, and 0.027 L mg⁻¹, 0.936, 0.959, and 0.989 for TSS, TDS, and P, respectively. The essential characteristics of the Langmuir isotherm parameters can be used to predict the affinity between the sorbate and sorbent using separation factor or dimensionless equilibrium parameter, R_L , provides important information about the nature of adsorption. The value of R_L indicated the type of Langmuir isotherm to be irreversible ($R_L = 0$), favorable ($0 < R_L < 1$), linear ($R_L = 1$) or unfavorable ($R_L > 1$). The R_L for (P, TSS, and TDS) adsorption by *P. australis* was found to be 0.6494–0.2703 for concentration of 20–100 mg L⁻¹ of P, 0.2613–0.0661 for concentration of 370–1,850 mg L⁻¹ of TSS, and 0.6745–0.1189 for concentration of 3,480–17,400 mg L⁻¹ of TDS. They are in the range of 0.0–1.0 that indicates the favorable adsorption.

3.7.2. Freundlich isotherm

Freundlich equilibrium constants were determined from the plot of $\ln q_e$ versus $\ln C_e$. The value of regression coefficients R^2 are 0.998, 0.999, and 0.999 for P, TSS, and TDS, respectively, which is regarded as a measure of goodness of fit of the experimental data to the isotherm models. The Freundlich model is more suitable than the Langmuir model for the representation of the adsorption data because it has higher R^2 values. The values of K_f and $1/n$ were 3.927, 3.381, and 1.45 mg g⁻¹ and 0.72, 0.7817, and 0.8712 L g⁻¹ for TSS, TDS, and P respectively.

3.8. Adsorption Kinetics

Adsorption kinetics contemplate is imperative in treatment of watery effluents as it gives profitable data on the response pathway and in the instrument of adsorption responses. A few active models are being used to clarify the instrument of the adsorption forms with a specific end goal to have the capacity to plan mechanical scale partition forms. To examine the instrument of adsorption, kinetic models have been abused to break down the experimental data. In addition, information on the kinetics of P, TSS, and TDS uptake is required to select the optimum condition for scaling up the P, TSS, and TDS removal processes. Several kinetic models such as pseudo-first-order, pseudo-second-order, and intraparticle diffusion model have been applied

Table 3

Parameters of the isotherm study (Langmuir and Freundlich models) and reaction kinetics (pseudo-first-order and pseudo-second-order) for TSS, TDS, and phosphorus biosorption using *Phragmites australis* (at room temperature of $25 \pm 3^\circ\text{C}$)

	Linear equation	Coefficients	r^2
Isotherm model			
Langmuir isotherm	$y_{\text{TSS}} = 0.004x + 0.5239$	$q_m = 250 \text{ mg g}^{-1}$ $K_1 = 0.00764 \text{ L mg}^{-1}$	0.936
	$y_{\text{TDS}} = 0.0004x + 0.9382$	$q_m = 2500 \text{ mg g}^{-1}$ $K_1 = 0.000426 \text{ L mg}^{-1}$	0.959
	$y_{\text{Phos}} = 0.0417x + 1.5341$	$q_m = 23.981 \text{ mg g}^{-1}$ $K_1 = 0.027 \text{ L mg}^{-1}$	0.989
R_L TSS	0.0661		
R_L TDS	0.1189		
R_L Phos.	0.2703		
Freundlich isotherm	$y_{\text{TSS}} = 0.72x + 1.3678$	$1/n = 0.72 \text{ L g}^{-1}$ $K_f = 3.927 \text{ mg g}^{-1}$	0.999
	$y_{\text{TDS}} = 0.7817x + 1.2183$	$1/n = 0.7817 \text{ L g}^{-1}$ $K_f = 3.381 \text{ mg g}^{-1}$	0.999
	$y_{\text{Phos}} = 0.8712x + 0.3717$	$1/n = 0.8712 \text{ L g}^{-1}$ $K_f = 1.45 \text{ mg g}^{-1}$	0.998
Reaction kinetics			
Pseudo-first-order	$y_{\text{TSS}} = -0.0148x + 2.0698$	$K_1 = 0.0341 \text{ mg g}^{-1} \text{ min}^{-1}$ $q_e = 117.436 \text{ mg g}^{-1}$	0.99
	$y_{\text{TDS}} = -0.0573x + 4.5378$	$K_1 = 0.132 \text{ mg g}^{-1} \text{ min}^{-1}$ $q_e = 34498.4831 \text{ mg g}^{-1}$	0.664
	$y_{\text{Phos}} = -0.0515x + 1.9945$	$K_1 = 0.1186 \text{ mg g}^{-1} \text{ min}^{-1}$ $q_e = 98.7416 \text{ mg g}^{-1}$	0.85
Pseudo-second-order	$y_{\text{TSS}} = 0.0076x + 0.2428$	$K_2 = 0.0002379 \text{ g mg}^{-1} \text{ min}^{-1}$ $q_e = 131.5789 \text{ mg g}^{-1}$	0.979
	$y_{\text{TDS}} = 0.0008x + 0.0324$	$K_2 = 0.0000198 \text{ g mg}^{-1} \text{ min}^{-1}$ $q_e = 1250 \text{ mg g}^{-1}$	0.947
	$y_{\text{Phos}} = 0.1534x + 3.2582$	$K_2 = 0.0072222 \text{ g mg}^{-1} \text{ min}^{-1}$ $q_e = 6.5189 \text{ mg g}^{-1}$	0.998

to investigate the adsorption mechanism [18]. The equations of the three kinetic models are expressed in Tables 3 and 4, supporting information. The corresponding linear parameters were presented in Table 3. Obviously, sorption of P, TSS, and TDS on the *P. australis* almost achieved to equilibrium within previous 120 min, indicating a high efficiency in sorbing P, TSS, and TDS.

The linear regression coefficients of the pseudo-second-order model were 0.998, 0.947 while they were 0.85, 0.664 for P and TDS of the pseudo-first-order model. The linear regression coefficients of the pseudo-second-order model were 0.979 while it was 0.99 for TSS of the pseudo-first-order model. Moreover, the calculated equilibrium sorption amounts for P and TDS by pseudo-second-order model were quite agreement with the experimental sorption amounts as shown in Table 3. The above facts indicate that sorption of P and TDS on the *P. australis* could be described well by

pseudo-second-model, representing the heterogeneous surfaces adsorption. This model portrays the substance idea of adsorption process, including the associations of valence powers or electron trade amongst adsorbent and adsorbate [18]. While TSS could be well suited by pseudo-first-order model representing the heterogeneous surfaces adsorption. Thus, the sorption mechanism is ascribed to physisorption, as opposed to chemisorptions. However, Weber and Morris intraparticle model cannot be ignored and the high-value determination coefficient to *P. australis* suggests that, in the first minutes, the adsorption processes also occurs significantly by intra-particle transport of P, TSS, and TDS to the inner pore by surface diffusion process. All processes reached the equilibrium at 120 min.

The intra-particle-diffusion model is constantly used to extensively show the adsorbate dispersion component and decide if intra-particle-diffusion is the rate-restricting

Table 4
Parameters of the intraparticle diffusion model for the adsorption of TSS, TDS, and phosphorus onto *Phragmites australis* at different initial concentrations

Adsorbates	C_0	K_{id}	C	R^2
P	100	0.3444	1.7397	0.8603
TSS	1,850	7.5475	21.607	0.8269
TDS	17,400	70.636	157.97	0.8313

variable controlling the adsorption procedure, particularly in a strong fluid adsorption framework. For intraparticle diffusion plots, the first portion indicates a boundary layer effect at the initial stage of the adsorption. The second portion of linear curve (shown in Fig. 12) is the gradual adsorption stage where intraparticle diffusion is the rate limiting. In some cases, the third portion exists, which is the final equilibrium stage where intraparticle diffusion starts to slow down due to the extremely low adsorbate concentrations left in the solutions. The determination coefficients of the whole process were all between 0.8603 and 0.8269, indicating that the intra-particle-diffusion model was not the only rate-limiting step; a multi-step process is expected to work during the entire time range. The linear plot for P, TSS, and TDS adsorption did not pass through the origin and could be divided into two stages according to the changing P, TSS, and TDS adsorption rate (Fig. 12). The first gradual adsorption stage region is instantaneous adsorption stage or the transport of P, TSS, and TDS molecules from the bulk solution to the adsorbent external surface driven by the initial P, TSS, and TDS gradients where intraparticle diffusion is the rate limiting. The second portion exists, which is the final equilibrium stage where intraparticle diffusion starts to slow down due to the extremely low adsorbate concentrations left in the solutions. The second portion is the intra-particle-diffusion process, P, TSS, and TDS molecules transported from external surface into the pores of *P. australis*, showing chemical sorption characteristic. The values of K_{id} and C were obtained from the linear portion. Table 4 shows the calculated intraparticle diffusion parameters for the adsorption process. Intraparticle diffusion equation yielded lower R^2 values when compared with the R^2 values of the first two equations. Previous researcher suggested that sorption system was chemical sorption involving valence forces through

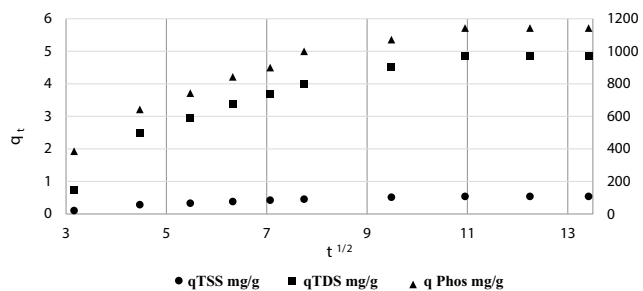


Fig. 12. Intraparticle diffusion kinetics for TSS, TDS, and phosphorus biosorption by *Phragmites australis* from industrial oil and soup ww at optimum conditions. ● qTSS mg g⁻¹; ■ qTDS mg g⁻¹; and ▲ q Phos mg g⁻¹

sharing or exchange of electrons between adsorbent and adsorbent when experimental data fit well with the pseudo-first-order model and pseudo-second-order model [24].

3.9. Biosorption to real wastewater samples

In this investigation, another type of real wastewater samples was collected from the olive mill wastewater effluent from El Fairoz factory in North Sinai governorate. Four samples were used to conduct biosorption experiments in triplicate at the optimum operating conditions as previously identified by oil and soup derivatives industrial wastewater batch experiments (pH 7.0; biosorbent dosage 14 g L⁻¹ (3.5 g per 250 mL); time 120 min; agitation speed 150 rpm; particle size 0.15 mm). The detected TSS and TDS concentration during Olive Mill Wastewater Oil, season 2017 was 1,430 and 41,820 mg L⁻¹, respectively. However, after biosorption, organic load TSS and TDS removal ratio in the four wastewater treatment plant samples was 91.3% and 87.4%, respectively. This result indicated that the investigated plant material *P. australis* (dried biomass) could be used as an efficient biosorbent for organic load TSS and TDS removal from polluted industrial wastewater. However, feasibility studies of the proposed system for application in real environmental field remain to be investigated; and that will be the focus of our future work.

3.10. Comparison with others materials

A great variety of different types of materials for P removal was described in previous studies. Authors as [28,29] listed around of 30 materials, categorized as: natural materials, industrial by-products and developed products that have been used as adsorbents for the P removal. Based on these studies, we can compare the yield of P removal of many materials with the *P. australis* material. Tables 5–7 show the efficiency reported for some materials with adsorption isotherm and kinetic studies, respectively, in removing P from water, in batch experiments. As per these examinations, materials, for example, Calcium flour biochar, fly fiery remains, ZIF-8 and Sun coral-based materials are considered among the best, in their particular classes. On the off chance that contrasted and these best materials, *P. australis* ends up being a decent alternative for P removal demonstrating the significance of finding locally accessible materials with high P maintenance limit with regards to use in wastewater treatment. *P. australis* possessed the fourth position in p evacuation limit as indicated by larger part of concentrates up to late [30]. *P. australis* is novel low-costs adsorbents represent a promising green technology. Furthermore, the majority of the studies published in literature focused on synthetic solutions with only few studies using real wastewater.

The outcomes uncovered that the adsorption of contemplated contaminations on crude *P. australis* was positive notwithstanding effectively managing and working with it. From metal material accessibility perspective, basic reed has been delegated a standout amongst the most adequate feedstock for esteem included item, due to its simple flexibility to various environmental conditions, high biomass profitability and capacity to escalated development. In this way, the utilization of *P. australis* for wastewater treatment

Table 5
Comparison between the study and previous studies for the biosorption of phosphorus from point of view of operating parameters

Type	Material	Variables pH, temperature, P total	Amount of P removed (mg g ⁻¹)	P removal (%)	Ref.
Sun coral powder	RSC (20 min)	6.58 27.4°C 1.71 mg L ⁻¹	6.826	78.17	[29]
	SCA (20 min)	6.58 27.4°C 1.71 mg L ⁻¹	7.062	79.14	
	SCQ (20 min)	6.58 27.4°C 1.71 mg L ⁻¹	9.597	98.64	
calcium-flour biochar	(Ca-BC) (2:1) (24 h)	7.20–12.3 25°C 350 mg L ⁻¹	314.22		[30]
hybrid adsorbent (metal-organic frameworks)	(ZIF-8) (30 min)	pH 2.8 Room temperature P: 10 mg L ⁻¹	38.22	88.9	[31]
Man-made products	Filtralite P TM (24 h)	pH 10.7 Phosphates: 0–480 ppm	2.5 g P kg ⁻¹		[32]
Man-made products	Leca (Estonian) (24 h)	pH 7.4 P 5–1000 mg PO ₄ L ⁻¹	0–10 mg P g ⁻¹ up to 7.98 mg P g ⁻¹		[28]
Man-made products	LWA (USA)	pH 10.1 P (0–320 mg L ⁻¹)	3465 mg P kg ⁻¹		[33]
Natural materials	Alunite (calcinated) (29.1 min)	pH 5 P (25–150 mg L ⁻¹)		Average of over 80% removal	[34]
Natural materials	Dolomite (24 h)	pH 7.8 P (0–100 mg L ⁻¹)	0.168 g P kg ⁻¹		[35]
Natural materials	Apatite (1–48 h)	P 0–500 mg L ⁻¹	4.76		[36]
Natural materials	Limestone	pH 8.9 P 5–25 mg PO ₄ -P L ⁻¹	0.25–0.3 mg P g ⁻¹		[37]
Industrial by-products	Ochre (15 min)	pH 7.2 P (1500 and 3000 mg P L ⁻¹)	0.026 g P kg ⁻¹	90%	[38,39]
Industrial by-products	Fly ash (24 h) coal power plant, China	pH 5 P 25–1000 mg L ⁻¹ ,	5.5 to 42.6 g P kg ⁻¹		[40]
Industrial by-products	Blast furnace slag	pH 7.7 P 0–320 mg L ⁻¹	9150 mg P kg ⁻¹		[41]
Industrial by-products	Red mud (6 h)	P 0–1 mg L ⁻¹	0.58		[42]
Dried biomass	<i>Phragmites australis</i> (2 h)	pH 7 P 20:100 mg L ⁻¹ Room temp. (25°C)	23.981	87%	This study

Table 6

Comparison between the study and previous studies for the biosorption of phosphorus from point of view of isotherm models

Adsorbent	Langmuir			Freundlich			Reference
	q_m (mg g ⁻¹)	K_L	r^2	K_F	n^{-1}	r^2	
RSC	6.826	0.7157	0.9979	1.4969	0.3161	0.8832	[29]
SCA	7.062	1.0351	0.9989	1.5631	0.3183	0.8523	[29]
SCQ	9.597	4.1513	0.9979	2.5513	0.0373	0.842	[29]
Granular Zeolite	3.29	0.29	0.9792	0.732	0.548	0.8944	[26]
Globular Zeolite	0.086	0.32	0.9835	0.0365	0.211	0.7078	[26]
Zeolitic imidazilate	38.22	0.94	0.99	640.3	0.2801	0.93	[32]
<i>P. australis</i>	23.981	0.027	0.989	1.45	0.8712	0.998	This Study

Table 7

Comparison between the study and previous studies for the biosorption of phosphorus from point of view of kinetics models

Adsorbent	Model	r^2	K_1 (mg g ⁻¹ min)	K_2 mg g ⁻¹ min)	K_{id}	Ref.
RSC	Pseudo-first-order	0.9206	0.3081	–	–	[29]
RSC	Pseudo-second-order	0.9944	–	0.1952	–	[29]
RSC	Weber and Morris	0.9823	–	–	1.259	[29]
SCA	Pseudo-first-order	0.9408	0.3560	–	–	[29]
SCA	Pseudo-second-order	0.9981	–	0.3431	–	[29]
SCA	Weber and Morris	0.9893	–	–	1.375	[29]
SCQ	Pseudo-first-order	0.9356	0.1960	–	–	[29]
SCQ	Pseudo-second-order	0.9993	–	0.1843	–	[29]
SCQ	Weber and Morris	0.8963	–	–	1.224	[29]
Zeolitic imidazilate	Pseudo-first-order	0.98	0.054	–	–	[31]
	Pseudo-second-order	0.99	–	0.003	–	[31]
	Weber and Morris	0.96	–	–	3.83	[31]
<i>P. australis</i>	Pseudo-first-order	0.85	0.1186	–	–	This Study
	Pseudo-second-order	0.998	–	0.00722	–	This Study
	Weber and Morris	0.8603	–	–	0.344	This Study

has been tended to by little investigations for its ability in colors, overwhelming metals and veterinary pharmaceuticals. Notwithstanding, different focuses are still should be explored like advancement of adjustment techniques, use of composite adsorbents, treatment of modern wastewaters, fascination of blended contaminants, settled bed studies, and recovery thinks about. The present authors think that the elaboration of simple methodological tools from financial and natural view, as portrayed in materials and strategies area in this investigation, planning of dried *P. australis* biomass powder cost no specified cash in contrast with readiness of different materials with change and added substances that cost much cash notwithstanding ecological unsafe added substances (chemicals) materials. Comparisons of P adsorbent using this metric indicates that the P removal costs by *P. australis* (estimated at 0.28–0.3 \$ g⁻¹ P removal; included harvesting and transportation cost = 0.1 \$ ± 0.05 \$ and electricity consumption 0.18 \$ ± 0.07 \$) in comparison with calcium-flour biochar (estimated at 5.6–6.0\$ g⁻¹ P removal).

3.11. IRSM models for P, TSS, and TDS

As listed in Table 8 positive linear effects of the independent variables “adsorbent dose,” “agitation speed,” and “contact time” on Phosphorous removal were observed to be significant ($p < 0.05$). Additionally, a significant negative effect ($p < 0.05$) was noticed for the quadratic term of “agitation speed,” and “contact time.” However, insignificant effects ($p > 0.05$) were determined for the linear terms of “initial P concentration,” and “pH,” as well as quadratic terms of “adsorbent dose,” “pH,” and “initial P concentration.” As listed in Tables 9 and 10, positive linear effects of the independent variables “adsorbent dose” and “contact time” on TSS and TDS removal were observed to be significant ($p < 0.05$). Additionally, a significant negative effect ($p < 0.05$) was noticed for the quadratic term of “contact time,” and “contact time”. However, insignificant effects ($p > 0.05$) were determined for the linear terms of “agitation speed,” “initial TSS&TDS concentration,” and “pH,” as well as quadratic terms of “adsorbent dose,”

Table 8
t statistics and *p*-values for coefficients of a pure-quadratic regression model (for phosphorus)

	Estimate	Standard error	<i>t</i> ratio	Prob > <i>t</i>	Effect
β_0	-55.5545	34.76439	-1.59803	0.124302	Insignificant
β_1	21.76	7.702586	2.825025	0.009858	Significant
β_2	0.61208	0.276933	2.210211	0.037796	Significant
β_3	0.817711	0.10225	7.997191	5.94E-08	Significant
β_4	-1.17741	6.645177	-0.17718	0.860986	Insignificant
β_5	0.194642	0.355278	0.54786	0.589304	Insignificant
β_6	-2.87189	1.73608	-1.65424	0.112278	Insignificant
β_7	-0.00183	0.000649	-2.82061	0.009958	Significant
β_8	-0.00305	0.000558	-5.46548	1.72E-05	Significant
β_9	0.081948	0.547415	0.149699	0.882366	Insignificant
β_{10}	-0.00239	0.002695	-0.88669	0.384837	Insignificant

Table 9
t statistics and *p*-values for coefficients of a pure-quadratic regression model (for TSS)

	Estimate	Standard error	<i>t</i> ratio	Prob > <i>t</i>	Effect
β_0	9.566908	44.22922973	0.216303	0.8307448	Insignificant
β_1	23.60204	9.799665492	2.408453	0.0248401	Significant
β_2	-0.08983	0.352329729	-0.25497	0.8011173	Insignificant
β_3	0.98213	0.130087991	7.549732	1.52E-07	Significant
β_4	1.893155	8.454370283	0.223926	0.8248811	Insignificant
β_5	0.009913	0.024432689	0.405708	0.6888756	Insignificant
β_6	-3.8796	2.208739783	-1.75648	0.0929198	Insignificant
β_7	-0.00043	0.000825119	-0.52143	0.6072753	Insignificant
β_8	-0.00373	0.000710192	-5.24915	2.89E-05	Significant
β_9	-0.12066	0.696452619	-0.17325	0.8640369	Insignificant
β_{10}	-7.15E-06	1.00E-05	-0.71387	0.4828132	Insignificant

Table 10
t statistics and *p*-values for coefficients of a pure-quadratic regression model (for TDS)

	Estimate	Standard error	<i>t</i> ratio	Prob > <i>t</i>	Effect
β_0	15.39331	44.8272094	0.343392	0.734563	Insignificant
β_1	25.56695	9.932157078	2.574159	0.017307	Significant
β_2	-0.17605	0.357093231	-0.49301	0.626892	Insignificant
β_3	0.955789	0.131846782	7.249242	2.91E-07	Significant
β_4	0.878314	8.568673463	0.102503	0.919286	Insignificant
β_5	0.000933	0.00263285	0.354398	0.726415	Insignificant
β_6	-4.29423	2.238601969	-1.91826	0.068148	Insignificant
β_7	-0.00023	0.000836275	-0.27893	0.782902	Insignificant
β_8	-0.00359	0.000719794	-4.98472	5.47E-05	Significant
β_9	0.014716	0.705868666	0.020848	0.983554	Insignificant
β_{10}	-7.43E-08	1.15E-07	-0.64702	0.524312	Insignificant

“agitation speed,” “pH” and “initial TSS&TDS concentration.” The coefficient of determination between measured data and simulated results (r^2), adjusted r^2 , and mean squared error was 0.9708, 0.9576, and 22.3276, 0.9623, 0.9451, and 36.1403, and 0.9620, 0.9447, and 37.1241 for P, TSS, and TDS, respectively. The high r^2 -value suggested the

reliability of the proposed model. For simplicity, the insignificant factors were excluded, and a new regression model was obtained (Eqs. (2)–(4)):

$$Y_p = -64.8861 + 21.93558X_1 + 0.627684X_2 + 0.850658X_3 - 2.92853X_1^2 - 0.0019X_2^2 - 0.0032X_3^2 \quad (2)$$

$$Y_{TSS} = -13.7174 + 23.51005X_1 + 0.964869X_3 - 3.84992X_1^2 - 0.00365X_3^2 \quad (3)$$

$$Y_{TDS} = -19.1465 + 25.66314X_1 + 0.973838X_3 - 4.325258X_1^2 - 0.00367038X_3^2 \quad (4)$$

where Y is the predicted response of P, TSS, and TDS removal efficiency (%); X_1 is adsorbent dose (20–100); X_2 is agitation speed (120–300 rpm); X_3 is contact time (10–180 min). The plot in Figs. 13–15 displays a contour of IRSM for P, TSS, and TDS removal efficiency against the independent variables, pH, initial P, TSS, and TDS concentration, time, agitation speed, and biomass dosage. The IRSM plots a 95% simultaneous

confidence band for the fitted response surface as two red curves. Independent variables are displayed in the text boxes on the horizontal axis and are marked by vertical dashed blue lines in the plots. The green line in Figs. 13–15 corresponds to the pure-quadratic regression models in Eqs. (2)–(4). The IRSM can be used to determine the P, TSS, and TDS removal efficiency at precise experimental parameters. For example, at pH 7, P, TSS, and TDS concentration 100, 1,850, and 17,400 mg L⁻¹, contact time 120 min, agitation speed 150 rpm, and biomass dosage 3.5 g, the predicted P, TSS, and TDS removal efficiency could be estimated as 81.6%, 86.9% and 84.3% for P, TSS, and TDS, respectively. This simulated P, TSS, and TDS removal efficiency were quite close to the

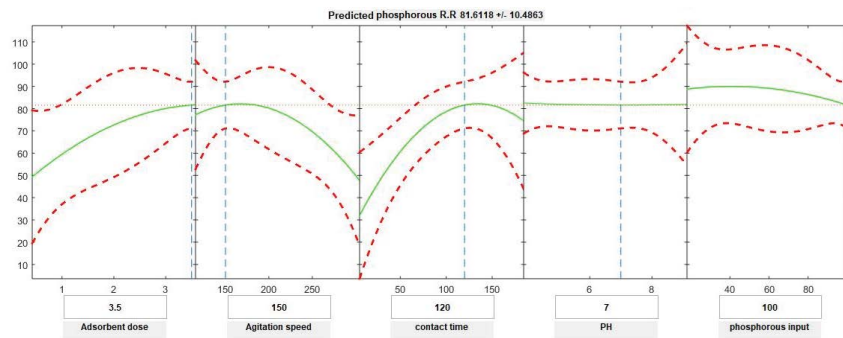


Fig. 13. Interactive response surface methodology for estimation of phosphorus removal efficiency using the independent variables: pH, initial phosphorus concentration, contact time, agitation speed, and biomass dosage.

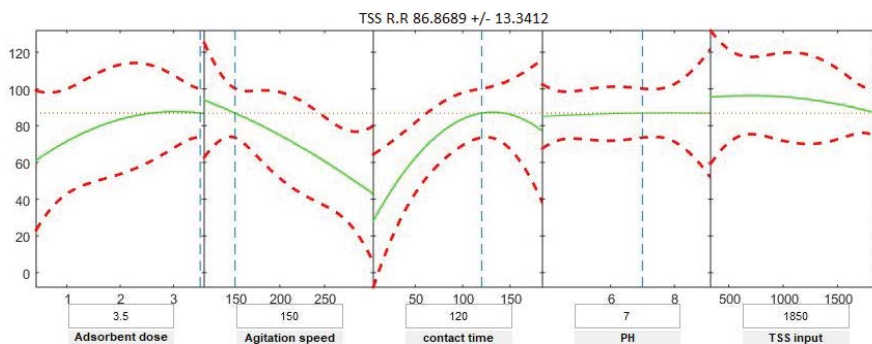


Fig. 14. Interactive response surface methodology for estimation of TSS removal efficiency using the independent variables: pH, initial TSS concentration, contact time, agitation speed, and biomass dosage.

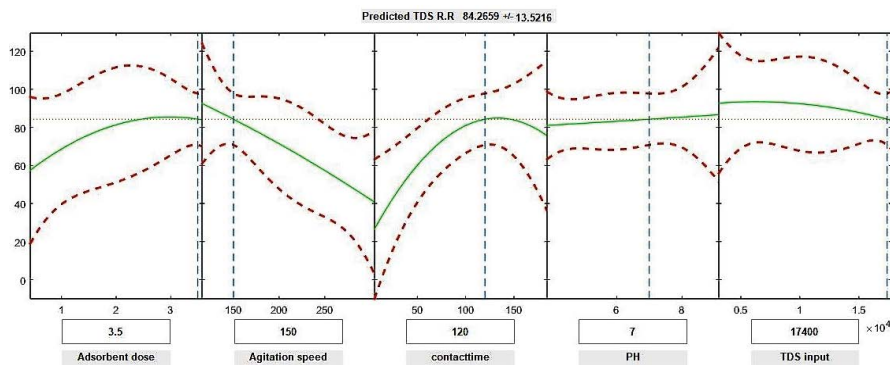


Fig. 15. Interactive response surface methodology for estimation of TDS removal efficiency using the independent variables: pH, initial TDS concentration, contact time, agitation speed, and biomass dosage.

actual record of 87%, 93.51%, and 90.22%, under the same experimental condition.

3.12. Vision for harvesting *P. australis* in real wastewater treatment plant

According to *P. australis* properties even in temperate areas, untreated stems of *P. australis* deteriorate within 10 years, but with correct harvesting and preservative treatment, its life expectancy can increase about tenfold. Mature stems have greater resistance to deterioration than younger ones. Stems are renewed each growing season. Growth can reach 4 cm d⁻¹. Rhizomes of *P. australis* live for 3–7 years, horizontal parts up to 12 years. Rhizomes contain an extensive horizontal and vertical aeration system allowing rapid metabolism. Although *P. australis* grows best on clay, it occurs in a wide variety of soils and tolerates moderate salinity. Stands in the Nile Delta – Egypt tolerate a soil pH of 7.0 – 9.3. Standing did material often totals twice as much biomass as current growth, allowing stands to burn even during the growing season. *P. australis* is a warm-season grass that starts growth after the last frost has occurred and rests green until frost in autumn and its well-known as wide climatic tolerance.

Harvesting is best done when seed has matured and when fine leaves have started to dry. Moisture content should also be as low as possible to minimize insect and fungal attacks. To take advantage of the most durable part of the stem, it should be cut as close to the ground as possible. The stems with cut ends aligned are loosely tied in small bundles and combed to remove debris and fine leaves. The straight hollow stems are cut in late autumn or winter and dried. In general, harvesting rises reed density, but also surges the amount of dead rhizomes while it decreases growth rate and shoot length and diameter. Usually, an area is selected and all *P. australis* within that area are harvested. The cut reed is sorted into bundles containing stems of even thickness and length. The taller and thicker stems are the most prized and of the highest quality. *P. australis* needs 1.6–2.0 ha to cover 140 m².

Handling after harvest is essential. Freshly cut stems, complete with leaves are tied into bundles and left standing for a few days, allowing the leaves to transpire and reduce the starch content of the stem. This method, called “clump curing,” reduces attack by borer beetles, but has no effect on termites or fungi. Effective resistance to termites, most types of fungus and fire is achieved mainly by chemical treatment. Dry, well-ventilated storage is essential [43]. Reed is one of the most frequent and dominant species in wetlands all over the world. Reed has been proofed to be beneficial for reducing the nutrient contents of water because it absorbs the nitrogen and phosphorus through its rhizomes during the growing season, which increased the N released during decomposition 4 to 7 fold. Reed cutting can in some cases remove the N&P from the wetland, which accelerate eutrophication by pumping up nutrients from the sediments. To save transportation costs and environment protection from gaseous emission by vehicles, the authors recommend reed harvest from wetlands near wastewater treatment plant [44].

3.13. Limitation to this study

Variation in characterization of industrial wastewater effluent attributed to the product type and processing

methods. The present study mainly focused on the main problem pollutant (P) of this oily wastewater and suggested an alternative treatment method for this type of industrial wastewater effluent before disposal to sewer lines, canal or open drain. This encourages the environment of meeting nitrogen and phosphorus for eutrophication. This study is basically focused on soap and oil wastewater before its disposal in sewer lines and surface water. The following reasons answer the question why this study did not investigate coexisting ions:

- The present study discussed the oil industry which does not contain heavy metals in its characterization analysis. This was in agreement with [45], who identified all oily industries contents.
- Examination with SEM after adsorption, demonstrated the adsorption sites of *P. australis* biomass remain unsaturated. This leads to the availability of the functional group for complexation of the metal ions.
- From FTIR analysis, *P. australis* contains cellulose, lignin, carbohydrates, and compound contents, which have metal-binding functional groups such as carboxyl, hydroxyl groups.
- The competition between phosphorus, cations, and anions mainly depends on the charge electrostatic attraction, hydration energy, hydrated radii of metal and electronic configuration.
- The Freundlich model fits the experimental data, Freundlich constant is widely acceptable in characterizing the metal sorption capacity of various materials. Thus indicative of the formation of multilayer adsorption and heterogeneous surface sites [46].

4. Conclusion

- FTIR revealed that the functional groups –OH, –CH, –C=O, –CH₃, C=H, C≡H, and C–OH were mainly involved in the biosorption of raising or lowering pH under the present range of the experimental condition onto *P. australis*.
- SEM showed that visualize the porous structure of *P. australis* and high affinity of *P. australis* to the direct organic loads, confirming the adsorption process. The surface texture of the examined plant was fluffy and rough, whereas after phosphorus, TSS, and TDS biosorption, they were coarse and crooked.
- Studying through different experimental parameters as adsorbent dose, contact time, pH, and agitation speed; the maximum removal efficiency of P, TSS, and TDS achieved at: adsorbent dosage = 14 gm L⁻¹; contact time = 120 min; pH = 7, and agitation speed = 150 rpm.
- From initial organic load concentration, revealed that increasing the initial P, TSS, and TDS could linearly decline the P removal from 89.54% ± 0.848% to 87.00% ± .820%, TSS removal from 96.43% ± 0.905% to 93.51% ± 1.325% and TDS removal from 93.54% ± 0.886% to 90.22% ± 1.273%.
- From the isotherm study, Langmuir and Freundlich models were applicable to the sorbent system, implying the existence of both monolayer and heterogeneous surface conditions. The biosorption of P, TSS, and TDS fitted well Freundlich isotherm with R² = 0.99.

- From sorption kinetics, the biosorption of P and TDS was in agreement with the pseudo-second-order model while the biosorption of TSS fitted well with pseudo-second order.
- IRSM was applied for phosphorus, TSS, and TDS, the predicted values were well coincides with the experimental results.

Comparing with these top materials, *P. australis* materials proves to be a good option for P, TSS, and TDS removal showing the importance of finding locally available materials with high P, TSS, and TDS retention capacity for use in wastewater treatment.

Acknowledgment

The authors express gratitude to the staff of employees of Environmental Engineering Laboratory – Faculty of engineering – Zagazig University.

List of Abbreviations

BOD	–	Biological Oxygen Demand
COD	–	Chemical Oxygen Demand
SS	–	Suspended Solids
DS	–	Dissolved Solids
O&G	–	Oil and Grease
TSS	–	Total Suspended Solids
TDS	–	Total Dissolved Solids
P	–	Phosphorus
RSC	–	Raw Sun Coral
SCA	–	Sun Coral (Physically modified)
SCQ	–	Sun Coral (Chemically modified)
Ca-BC	–	Calcium-flour Bio Char
ZIF-8	–	Zeolitic Imidazolate Framework-8

References

- [1] C. Han, Z. Wang, W. Yang, Q. Wu, H. Yang, X. Xue, Effects of pH on phosphorus removal capacities of basic oxygen furnace slag, *Ecol. Eng.*, 89 (2016) 1–6.
- [2] Y.V. Nancharaiyah, M.S. Venkata, P.N.L. Lens, Recent advances in nutrient removal and recovery in biological and bio-electrochemical systems, *Bioresour. Technol.*, 215 (2016) 173–185.
- [3] D.D. Nguyen, H.H. Ngo, W. Guo, T.T. Nguyen, S.W. Chang, A. Jang, Y.S. Yoon, Can electrocoagulation process be an appropriate technology for phosphorus removal from municipal wastewater?, *Sci. Total Environ.*, 549–564 (2016) 549–564.
- [4] J. Rai, D. Kumar, L.K. Pandey, A. Yadav, J.P. Gaur, Potential of cyanobacterial biofilms in phosphate removal and biomass production, *J. Environ. Manage.*, 177 (2016) 138–144.
- [5] A. Oehmen, R.J. Zeng, Z. Yuan, Modeling the aerobic metabolism of polyphosphate-accumulating organisms enriched with propionate as a carbon source, *Water Environ. Res.*, 79 (2007) 2477–2486.
- [6] T. Panswad, A. Doungchai, J. Anotai, Temperature effect on microbial community of enhanced biological phosphorus removal system, *Water Res.*, 37 (2003) 409–415.
- [7] S.H. Lee, R. Kumar, B.H. Jeon, Struvite precipitation under changing ionic conditions in synthetic wastewater: experiment and modeling, *J. Colloid. Int. Sci.*, 474 (2016) 93–102.
- [8] E. Oguz, Removal of phosphate from aqueous solution with blast furnace slag, *J. Hazard. Mater.*, 114 (2004) 131–137.
- [9] N.Y. Acelas, B.D. Martin, D. López, B. Jefferson, Selective removal of phosphate from wastewater using hydrated metal oxides dispersed within anionic exchange media, *Chemosphere*, 119 (2015) 1353–1360.
- [10] P. Loganathan, S. Vigneswaran, J. Kandasamy, N.S. Bolan, Removal and recovery of phosphate from water using sorption, *Crit. Rev. Environ. Sci. Technol.*, 44 (2014) 847–907.
- [11] P. Kumar, I. Mehrotra, T. Viraraghavan, Temperature response of biological phosphorus removing activated return sludge, *J. Environ. Eng.*, 124 (1998) 192–196.
- [12] Egyptian Code of Environmental Regulations Appendix No. (1), (1982) (4/1994) 106–108.
- [13] B.C. Ahmed, P.K. Ghosh, G. Gajalakshmi, Total dissolved solids removal by electrochemical ion exchange (EIX) process, *Electrochim. Acta.*, 54 (2008) 474–483.
- [14] B.K. Gökben, U.M. Aysegül, T. İlhami, *Phragmites australis*: An alternative biosorbent for basic dye removal, *Ecol. Eng.*, 86 (2016) 85–94.
- [15] J. Srivastava, S.J.S. Kalra, R. Naraian, Environmental perspectives of *Phragmites australis* (Cav.) Trin. Ex. Steudel, *Appl Water Sci.*, 4 (2014) 193–202.
- [16] I. Langmuir, The adsorption of gases on plane surfaces of glass, mica and platinum [J], *J Am Chem Soc.*, 40 (1918) 1361–1368.
- [17] H. Freundlich, Adsorption in solution [J], *Phys Chem Soc.*, 40 (1906) 1361–1368.
- [18] Y.S. Ho, G. McKay, Pseudo-second order model for sorption processes, *Process Biochem.*, 34 (1999) 451–465.
- [19] W.J. Weber, J.C. Morris, Kinetics of adsorption on carbon from solution, *J Sanit Eng Div Am. Soc. Civ. Eng.*, 89 (1963) 31–60.
- [20] M.G. Alalm, M. Nasr, S. Ookawara, Assessment of a novel spiral hydraulic flocculation/sedimentation system by CFD simulation fuzzy inference system and response surface methodology, *Sep. Purif. Technol.*, 169 (2016) 137–150.
- [21] H. Sutcu, Pyrolysis of *Phragmites australis* and characterization of liquid and solid products, *J. Ind. Eng. Chem.*, 14 (2008) 573–577.
- [22] A.J. Romero-Anaya, M.A. Lillo-Roidenas, A. Linares-Solano, Factors governing the adsorption of ethanol on spherical activated carbons, *Carbon*, 83 (2015) 240–249.
- [23] V. Nair, A. Panigrahy, R. Vinu, Development of novel chitosan-lignin composites for adsorption of dyes and metal ions from wastewater, *Chem. Eng. J.*, 254 (2014) 491–502.
- [24] H. Yin, Y. Yun, Y. Zhang, C. Fan, Phosphate removal from wastewaters by a naturally occurring, calcium-rich sepiolite, *J. Hazard. Mater.*, 198 (2011) 362–369.
- [25] Y. Zhang, X. Kou, H. Lu, X. Lv, The feasibility of adopting zeolite in phosphorus removal from aqueous solutions, *Desal. Water Treat.*, 52 (2014) 4298–4304.
- [26] A.J. Maher, D. Hiba, Z. Nareman, E. Nadia, Reducing organic pollution of wastewater from milk processing industry by adsorption on marlstone particles, *Int. J. Thermal Environ. Eng.*, 15 (2017) 57–61.
- [27] A.L. Ahmad, S. Sumathi, B.H. Hameed, Residual oil and suspended solid removal using natural adsorbents chitosan, bentonite and activated carbon: A comparative study, *Chem. Eng. J.*, 108 (2005) 179–185.
- [28] C. Vohla, E. Poldvere, A. Noorvee, V. Kuusemets, U. Mander, Alternative filter media for phosphorus removal in a horizontal subsurface flow constructed wetland, *J. Environ. Sci. Health A*, 40 (2005) 1251–1264.
- [29] M.T.G. Vianna, M. Marques, L.C. Bertolino, Sun coral powder as adsorbent: Evaluation of phosphorus removal in synthetic and real wastewater, *Ecol. Eng.*, 97 (2016) 13–22.
- [30] S. Wang, L. Kong, J. Long, M. Su, Z. Diao, X. Chang, D. Chen, G. Song, K. Shih, Adsorption of phosphorus by calcium-flour biochar: Isotherm, kinetic and transformation studies, *Chemosphere*, 195 (2018) 666–672.
- [31] M. Shams, M.H. Dehghani, R. Nabizadeh, A. Mesdaghinia, M. Alimohammadi, A.A. Najafpoor, Adsorption of phosphorus from aqueous solution by cubic zeolitic imidazolate framework-8: Modeling, mechanical agitation versus sonication, *J. Molec. Liq.*, 224 (2016) 151–157.
- [32] K. Adam, T. Krogstad, F.R.D. Suliman, P.D. Jenssen, Phosphorus sorption by Filtralite-PTM – small-scale box experiment, *J. Environ. Sci. Health A*, 40 (2005) 1239–1250.

- [33] T. Zhu, P.D. Jenssen, T. Mahlum, T. Krogstad, Phosphorus sorption and chemical characteristics of lightweight aggregates (LWA)—potential filter media in treatment wetlands, *Water Sci. Technol.*, 35 (1997) 103–108.
- [34] M. Ozacar, Contact time optimization of two-stage batch adsorber design using second-order kinetic model for the adsorption of phosphate onto alunite, *J. Hazard. Mater. B*, 137 (2006) 218–225.
- [35] C.A. Prochaska, A.I. Zouboulis, Removal of phosphates by pilot vertical-flow constructed wetlands using a mixture of sand and dolomite as substrate, *Ecol. Eng.*, 26 (2006) 293–303.
- [36] P. Molle, A. Lienard, A. Grasmick, A. Iwema, A. Kabbabi, Apatite as an interesting seed to remove phosphorus from wastewater in constructed wetlands, *Water Sci. Technol.*, 51 (2005) 193–203.
- [37] L. Johansson, Industrial by-products and natural substrata as phosphorus sorbents, *Environ. Technol.*, 20 (1999a) 309–316.
- [38] K.V. Heal, P.L. Younger, K.A. Smith, S. Glendinning, P. Quinn, K.E. Dobbie, Novel use of ochre from mine water treatment plants to reduce point and diffuse phosphorus pollution, *Land Contam. Reclam.*, 11 (2003) 145–152.
- [39] K.V. Heal, K.E. Dobbie, E. Bozika, H. McHaffie, A.E. Simpson, K.A. Smith, Enhancing phosphorus removal in constructed wetlands with ochre from mine drainage treatment, *Water Sci. Technol.*, 51 (2005) 275–282.
- [40] J. Chen, H. Kong, W. Wu, X. Chen, D. Zhang, Z. Sun, Phosphate immobilization from aqueous solution by fly ashes in relation to their composition, *J. Hazard. Mater. B*, 139 (2007) 293–300.
- [41] E.A. Korkusuz, M. Beklioglu, G.N. Demirer, Use of blast furnace granulated slag as a substrate in vertical flow reed beds: field application, *Bioresour. Technol.*, 98 (2007) 2089–2101.
- [42] W.W. Huang, S.B. Wang, Z.H. Zhu, L. Li, X.D. Yao, V. Rudolph, F. Haghseresht, Phosphate removal from wastewater using red mud, *J. Hazard. Mater.*, 158 (2008) 35–42.
- [43] M. Brink, E.G. Achigan-Dako, *Plant Resources of Tropical Africa 16, Fibers*, PROTA Foundation/CTA, Wageningen, Netherlands, 2012.
- [44] J.F. Köbbing, N. Thevs, S. Zerbe, Cutting of *Phragmites australis* as a lake restoration technique: Productivity calculation and nutrient removal in Wuliangshuai Lake, northern China, *Sciences in Cold and Arid Regions*, 8 (2016) 35–47.
- [45] A.D. Patwardhan, *Industrial wastewater treatment*, Mumbai, 2008.